

Influence of defects on the electronic and magnetic properties of half-metallic CrAs, CrSe and CrSb zinc-blende compounds

I Galanakis and S G Pouliasis

Department of Materials Science, School of Natural Sciences, University of Patras, Patras 265 04, Greece

E-mail: galanakis@upatras.gr

Abstract. We present an extended study of single impurity atoms and atomic swaps in half-metallic CrAs, CrSb and CrSe zinc-blende compounds. Although the perfect alloys present a rather large gap in the minority-spin band, all defects under study, with the exception of void impurities at Cr and sp sites and Cr impurities at sp sites (as long as no swap occurs), induce new states within the gap. The Fermi level can be pinned within these new minority states depending on the lattice constant used for the calculations and the electronegativity of the sp atoms. Although these impurity states are localized in space around the impurity atoms and very fast we regain the bulk behavior, their interaction can lead to wide bands within the gap and thus loss of the half-metallic character.

PACS numbers: 75.47.Np, 75.50.Cc, 75.30.Et

Submitted to: *J. Phys. D: Appl. Phys.*

1. Introduction

The rapid emergence of the field of spintronics (also known as magnetoelectronics [1]) brought to the center of scientific research the so-called half-metallic ferromagnets (like Heusler alloys [2, 3, 4] or some oxides [5]). These compounds present metallic behavior for one spin-band while they are semiconducting or insulators for the other spin-band, resulting to perfect spin-polarization, at least for the bulk, at the Fermi level. Except Heusler and oxides, also transition-metal chalcogenides like CrAs or CrSb and pnictides like CrSe are known to present half-metallic ferromagnetism when they crystallize in the metastable zinc-blende structure. The first experimental evidence was provided in the case of CrAs thin-films by the group of Akinaga in 2000 [6] and many more experiments have confirmed these results [7]. Experiments agree with prediction of ab-initio calculations performed by several groups [8, 9, 10, 11]. In the case of the half-metallic ferromagnets like CrAs or CrSe, the gap in the minority-spin band arises from the hybridization between the p-states of the *sp* atom and the triple-degenerated t_{2g} states of the transition-metal and as a result the total spin-moment, M_t , follows the Slater-Pauling (SP) behavior being equal in μ_B to $Z_t - 8$ where Z_t the total number of valence electrons in the unit cell [8]. Recently theoretical works have appeared attacking also some crucial aspects of these alloys like the exchange bias in ferro-/antiferromagnetic interfaces [12], the stability of the zinc-blende structure [13], the dynamical correlations [14], the interfaces with semiconductors [15], the exchange interaction [16] and the temperature effects [17]. An extended overview on the properties of these alloys can be found in reference [18].

In a recent publication [19], it was shown using the coherent potential approximation [20] that for several com-

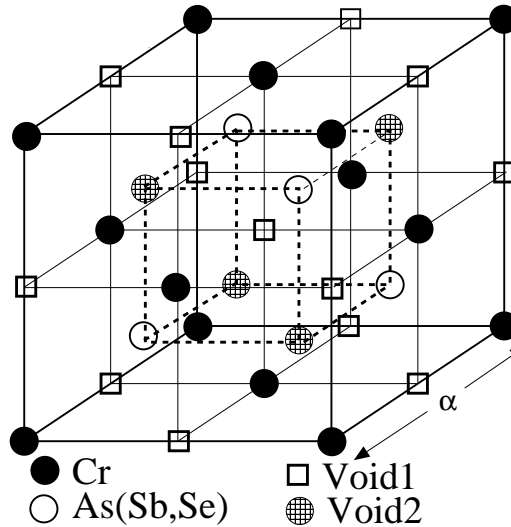


Figure 1. Schematic representation of the zinc-blende structure. To model the system in our calculations we assume the existence of two non-equivalent vacant sites. The lattice consists of 4 fcc sublattices. The unit cell is that of an fcc lattice with four atoms per unit cell: Cr at (000), As(Sb or Se) at $(\frac{1}{4} \frac{1}{4} \frac{1}{4})$ and the two vacant sites at $(\frac{1}{2} \frac{1}{2} \frac{1}{2})$ (Void1) and $(\frac{3}{4} \frac{3}{4} \frac{3}{4})$ (Void2).

pounds (like CrAs, CrSb and CrSe) an excess of the transition metal atoms leads to half-metallic ferrimagnetism [21]; Cr-impurities occupying sites occupied by the *sp* atoms in the perfect bulk compound couple antiferromagnetically to the existing Cr atoms at the ideal sites and destroy ferromagnetism keeping the half-metallic character of the parent compounds. Later in reference [22] it was shown that this also true when instead of Cr-impurities we introduce other transition metal atoms like V and Mn.

CPA is an average method and does not provide details on the nature of the single impurities. In this contribution we study in detail the role of single impurities taking into account not only the case

Table 1. Total and atom-resolved spin magnetic moments in μ_B for all four compounds under study. CrAs(GaAs) corresponds to CrAs studied for the experimental lattice constant of GaAs (0.565 nm) while (InAs) corresponds to the experimental lattice constant of InAs of 0.606 nm.

	CrAs(GaAs)	CrAs(InAs)	CrSb(InAs)	CrSe(InAs)
Cr	3.017	3.267	3.148	3.825
As(Sb,Se)	-0.198	-0.382	-0.249	-0.103
Void1	0.005	-0.029	-0.036	0.049
Void2	0.122	0.080	0.084	0.162
TOTAL	2.946	2.936	2.946	3.933

of Cr antisites but all possible defects in half-metallic zinc-blende compounds covering also the cases of atomic swaps between nearest neighbors. We have selected as test cases CrAs which is the most widely studied alloy, CrSb which is isovalent to CrAs and CrSe which has one electron more. We decided to use as lattice constant the experimental one of InAs of 0.606nm. As it was shown in reference [8] using the Korringa-Kohn-Rostoker method (KKR) for this lattice constant all three alloys are half-metals with the Fermi level exactly at the middle of the gap and thus the effect of defect states is more visible. The half-metallicity is reflected on the total spin-moments which should be $3 \mu_B$ for CrAs and CrSb and $4 \mu_B$ for CrSe. As shown in table 1 the calculated total spin moments are close to these values and small deviations are due to the ℓ -cutoff used in the calculations [4]. We have also decided to study a fourth case: CrAs at the experimental lattice constant of GaAs (0.565 nm) which is a usual substrate for thin films of this alloy. The latter one is also half-metallic with the Fermi level near the right edge of the gap.

To perform our impurity calculations we have used a special implementation of the KKR method [23, 24]. First, a self-consistent calculation is performed for the perfect compound and the Green function is calculated and stored. Then we consider an impurity cluster embedded in the perfect crystal. We use the calculated

Green function for the infinite host crystal and we calculate self-consistently the electronic structure of the impurity cluster in the real space using the Dyson equation. In our case we found that an impurity cluster of 65 atoms is enough to converge the spin magnetic moment of single impurity atoms at the center of the cluster and atomic swaps between nearest neighboring atoms, but not to calculate also the energetics of the defects. Our available computer sources did not allow us to converge also the energetics with the size of the cluster. Within the impurity cluster the impurity states survived up to the second neighbors and in all cases we regained the perfect crystal behavior after the third neighbors.

The structure of the perfect crystal is shown in figure 1. The lattice is that of a fcc with four sites per unit cell. We take into account two vacant sites to represent adequately the zinc-blende structure. In other intermetallic compounds like the full-Heusler alloys these two sites are occupied [4]. We assign the names Void1 and Void2 to the two vacant sites in order to study the case of Cr and sp impurities at these sites. If we ignore the different chemical elements the lattice is in reality a bcc one. Each Cr atom is at the center of a cube with four sp atoms and four Void2 sites as first neighbors. The Void1 sites have the same local environment as the Cr sites rotated by 90° degrees. Similarly each sp atom and Void2 site are at a center of a cube with four Cr atoms and four

Table 2. Structure of the impurity cluster which in total contains 65 atoms. In parenthesis the distance between the *i*th neighbors and the center atom in units of the lattice constant.

Center	Cr	As	Void1	Void2
1st (0.433013)	4 As, 4 Void2	4 Cr, 4 Void1	4 As, 4 Void2	4 Cr, 4 Void1
2nd (0.500000)	6 Void1	6 Void2	6 Cr	6 As
3rd (0.707107)	12 Cr	12 As	12 Void1	12 Void2
4th (0.829156)	12 As, 12 Void2	12 Cr, 12 Void1	12 As, 12 Void2	12 Cr, 12 Void1
5th (0.866025)	8 Void1	8 Void2	8 Cr	8 As
6th (1.000000)	6 Cr	6 As	6 Void1	6 Void2

Void1 sites are nearest neighbors. When we create the impurity cluster we choose one of the four sites -Cr, sp atom, Void1 and Void2- at the center of the cluster and in table 2 we present the structure of the impurity cluster for all four cases. We can see that the clusters with Cr and Void1 sites at their center are not identical since they have the same 1st and 4th neighbor only which involve the sp and Void2 sites. The same occurs for the clusters with a sp atom or a Void2 site at their center. When we create an impurity we substitute the atom at the center of the cluster and recalculate the electronic and magnetic properties of the cluster. Similarly when we create an atomic swap we exchange the atom at the center of the cluster with one of each nearest neighbors.

In section 2 we present the case of Cr impurities at nearest neighboring sp or Void2 sites and in section 3 the case of sp impurities at nearest neighboring Cr or Void1 sites. In section 4 we discuss the other possible single impurities and in section 5 we discuss the case of atomic swaps between nearest neighboring atoms. Finally in section 6 we summarize and conclude. We should also mention here that in table 1 we present the atom-resolved spin moments for all four perfect bulk compounds under study to use them as a reference when discussing the spin magnetic moment of the impurities atoms (see reference [8] for an extended discussion of their behavior). Moreover to distinguish the two cases of CrAs we use

the notation "(GaAs)" for the case of the GaAs experimental lattice constant and "(InAs)" for the InAs experimental lattice constant.

2. Cr impurities at nearest neighbors sites

We will start our discussion from the case of Cr single impurities at nearest neighboring sites since in references [19] and [22] it was shown that Cr impurities at sites occupied by the sp atom in the perfect crystal lead to half-metallic ferrimagnetism. The Cr impurity atom has four Cr atoms and four Void1 sites as first neighbors. The distance is so short that the antiferromagnetic (AFM) coupling is favored between the spin magnetic moment of the impurity atom and its closest Cr neighbors. This is not surprising since it is well-known that both Cr and Mn atoms show AFM or ferromagnetic (FM) coupling of their spin moments depending on the distance between the neighboring transition metal atoms. In our study we have expanded it to cover also the case when Cr impurities appear at Void2 sites where the local environment is the same as for Cr impurities at sp atom sites.

In both cases of single Cr impurities, we found that depending on the starting potential we were able to converge to two different states: an antiferromagnetic one as in CPA calculations and a FM one. This can be seen in table 3 where

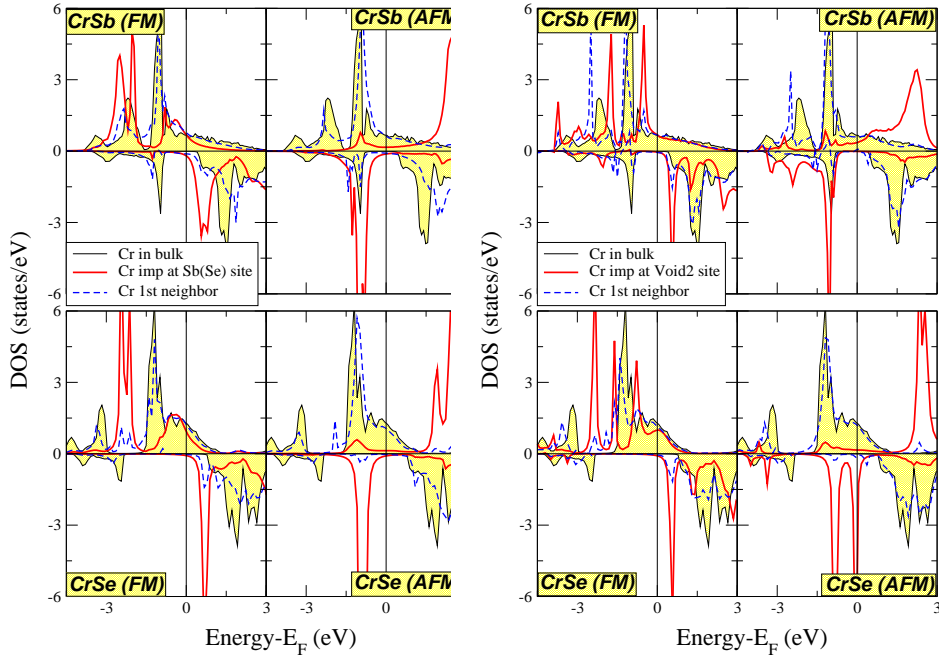


Figure 2. (Color online) Cr-resolved DOS for the case of Cr impurity atoms at Sb(Se) sites in the left panel and at Void2 sites in the right panel (solid red lines) and their Cr first neighbors (dashed blue lines) with respect to the perfect bulk case (solid black line with shaded region). We present both cases of ferromagnetic (FM) and antiferromagnetic (AFM) coupling of the Cr impurity spin moment (see text for details). The Fermi energy has been set as the zero of the energy axis. Positive DOS values correspond to the spin-up (majority-spin) electrons and negative values to the spin-down (minority-spin) electrons.

we present the spin magnetic moments of the Cr impurity atoms and their first neighbors. A close look at the energies shows that the AFM state is more favorable energetically with respect to the FM case (we were not able to converge the energy difference with the size of the cluster but the total energy difference was of the order of some eV). We will discuss also the FM case since in real situations this state can occur either due to the method used to grow the samples or due to an external field. We should also note here that although we have tried we were not able to get a FM solution for the case of CrAs at the GaAs lattice constant. GaAs lattice constant is considerably smaller with respect to the InAs lattice constant and thus the

distance between the Cr impurity atom and its first neighbors become much smaller and the FM solution becomes completely unstable. Thus the possibility of the FM coupling to occur depends strongly on the lattice constant. For the compounds under study their lattice constant is imposed by the substrate used to grow the films and thus we can exclude the FM coupling to appear by choosing a suitable substrate.

First, we will shortly discuss the FM case. In figure 3 we have plotted the DOS of the Cr impurity atoms at Sb(Se) and Void2 sites and their first Cr neighbors with respect to the Cr DOS in the perfect bulk CrSb and CrSe alloys (CrAs shows similar behavior). The Cr impurity atoms have now four Cr atoms as first neighbors

Table 3. Atom-resolved spin magnetic moments for the case of Cr impurity atoms at As(Sb or Se) and Void2 sites, and the case of Cr-As(Sb or Se) and Cr-Void2 atomic swaps. "imp" stands for impurity and "nn" stands for nearest neighbor atoms (1st neighbors). We present results for both cases of coupling of the Cr impurity spin moment with respect to the spin moments of the other Cr atoms (ferromagnetic-FM and antiferromagnetic-AFM cases).

	CrAs(GaAs)	CrAs(InAs)		CrSb(InAs)		CrSe(InAs)	
	AFM	FM	AFM	FM	AFM	FM	AFM
Cr impurity at As(Sb or Se) site							
Cr imp	-2.896	4.388	-3.690	4.504	-3.718	4.511	-3.642
Cr nn	2.985	3.602	3.364	3.537	3.301	3.994	3.715
Cr impurity at Void2 site							
Cr imp	-1.129	3.901	-2.908	3.854	-2.689	4.354	-3.350
Cr nn	2.779	3.419	3.267	3.316	3.175	3.941	3.703
Cr-As(Sb or Se) atomic swaps							
Cr imp	-2.840	4.098	-3.496	4.204	-3.558	4.037	-3.405
sp imp	0.118	0.075	0.162	-0.326	-0.325	-0.055	0.283
Cr-Void2 atomic swaps							
Cr imp	-2.224	3.851	-3.240	3.787	-3.157	4.241	-3.549
Void2 imp	-0.045	-0.060	-0.098	-0.057	-0.077	0.024	-0.027

instead of four Sb or Se atoms. The d electrons of the Cr impurity atoms now can hybridize with the d electrons of the neighboring atoms instead of the p electrons of the sp atom (only the triple degenerated t_{2g} electrons of Cr can couple to the p orbital of the sp atom). The majority-spin electrons of the Cr impurity are fixed in energy range since they form a common band with the other Cr atoms but the center of the majority band is shifted lower in energy. This leads to a shift of the unoccupied minority-spin states lower in energy, since the exchange splitting is comparable for all Cr atoms, and they become more localized in energy. The small weight of the occupied minority electrons vanishes since it was due to the hybridization with the p states of the sp atom. The shift the unoccupied minority band is such that the gap is scarcely affected and the half-metallicity is not destroyed. The Cr first neighbors show a DOS very similar to the bulk case since they have one Cr and three sp atoms as first neighbors and the effect of the Cr impurity atom on their properties is

weak. There is no significant difference whether the Cr impurity atom is located at the sp or Void2 site. Majority states are identical. In the minority-spin band the e_g states are located bear the Fermi level (the large pick just above the Fermi level). In the case of Cr impurity atoms at the sp sites the minority t_{2g} states overlap with the e_g states while in the case of Cr impurity atoms at the Void2 sites the unoccupied minority t_{2g} states are slightly higher in energy. The spin moments presented in table 1 do not show any unexpected behavior. The Cr impurity atoms have a larger spin moment with respect to the Cr atoms in the bulk case since the weight of the minority occupied states has vanished as a result of the hybridization with its first neighbors. The Cr atoms which are first neighbors of the impurity atoms present spin moments almost identical to the perfect compounds in table 1.

The second and most interesting case is the AFM coupling between the Cr impurity atom and the spin magnetic moments of its nearest Cr neighbors

since this is susceptible of leading to half metallic ferrimagnetism. This is crucial for applications since ferrimagnets create smaller external fields and thus exhibit smaller energy losses with respect to ferromagnets. In figure 2 we present also the cases of AFM coupling for Cr impurity at Sb(Se) and Void2 sites in CrSb and CrSe alloys. In the case where the Cr impurity atom is located at the sp atom site there is a very intense pick in the minority spin band which is occupied. This pick contains the 5 occupied bonding d states of the Cr impurity atom. But the spin magnetic moment of the impurity atom is not $-5 \mu_B$ but around -3 to $-3.5 \mu_B$. This is due to the majority t_{2g} bands which are very extended in energy and which are partially occupied due to their hybridization with the t_{2g} bands of the nearest neighboring d bands.

When the Cr impurity atom is located at the Void2 site the situation is more complex. While for CrSb the situation is similar to the case of the Cr impurity at the sp atom, for the other three compounds there is now a double pick structure in the spin-down band and the Fermi level falls within the second pick. This is also reflected on the spin moments of the Cr impurity atom, the absolute values of which are decreased with respect to the case of the Cr-impurity at the sp atom site (in the case of CrAs in the GaAs lattice constant the decrease is larger since also the weight of the spin-up states increases slightly). The magnitude of the decrease depends on the exact position of the Fermi level within the pick. To elucidate this behavior we have plotted in figure 3 the projection of the d states on the triple-degenerated t_{2g} electrons and on the double-degenerated e_g states for the case of CrAs in the InAs lattice constant. The t_{2g} states are more delocalized and couple to the p states of the sp atoms and thus are more extended in energy. On the other hand the e_g states can not couple to the p states of

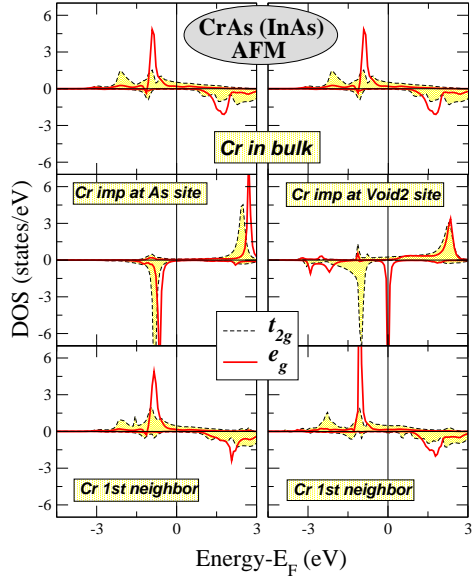


Figure 3. (Color online) Upper panel: Cr d -DOS decomposed on the e_g and t_{2g} orbitals for the bulk CrAs alloy at the InAs lattice constant; middle and lower panel: same for the case of AFM coupling of Cr impurity atoms at As (left panel) and Void2 (right panel) sites and their first Cr neighbors.

the sp atoms and are more localized in energy. This is reflected on the DOS of the Cr atom in the perfect crystal presented in the upper panel of figure 3 where the t_{2g} are more extended in energy. When we create the impurity at the As site we see that in the minority spin band the t_{2g} and e_g states almost overlap, while in the case of the Cr impurity at the Void2 site the e_g states move higher in energy and they are now located at the Fermi level. There is no immediate explanation for this behavior since it should be attributed to the different structure of the impurity clusters and not to the immediate environment of the impurity atoms. Cr impurities have in both cases 4 Cr atoms and four Void sites as first neighbors (the Cr neighboring atoms have

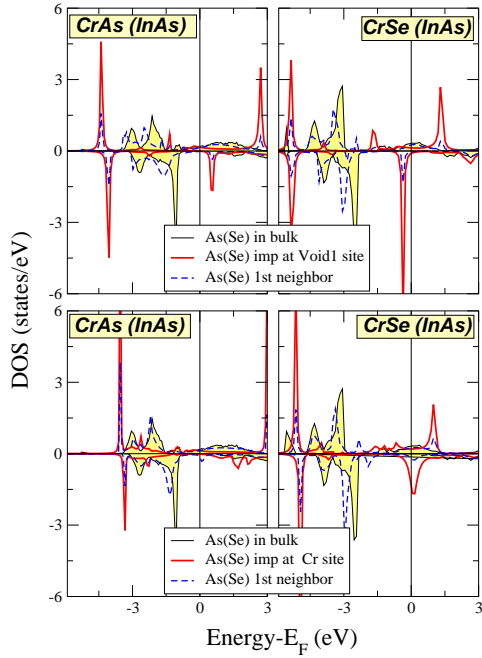


Figure 4. (Color online) As(Se)-resolved DOS for the case of As(Se) impurity atoms (solid red lines) and their 1st neighbors (dashed blue lines) for the case of As(Se) impurities at Void1 sites in the upper panel and Cr sites in the lower panel with respect to the perfect bulk case (solid black line with shaded region).

the same DOS and spin moments for both cases) but when the impurity is located at the As site, it has 12 As atoms as 3rd neighbors while when it is located at the Void2 site it has 6 As atoms as 2nd neighbors. This difference probably drives the shift of the minority e_g states. In the case of CrSb the shift is smaller leading to a more narrow and more intense pick in the minority spina band in the case of the Cr impurity at the Void2 site with respect to the case of the Cr impurity at the Sb atom.

3. sp impurities at nearest neighbors sites

We will continue our study with the case of sp impurities at the neighboring Cr and Void1 sites. The s electrons of the sp atoms are located very low in energy, at around -10 eV, and play no role to half-metallicity but this is not the case for the p electrons. In figure 4 we have plotted the DOS for both case of As(Se) impurities at Void1 and Cr sites with respect to the bulk CrAs and CrSe alloys. For both perfect bulk alloys the minority p states of As(Se) are completely occupied leading to small negative spin moments as can be seen in table 1. When the As(Se) atoms migrate to Cr or Void1 site they have four other As(Se) atoms and four Void2 sites as nearest neighbors. Thus the p states of the As(Se) impurity atoms have to hybridize with the p states of the neighboring As(Se) atoms which are almost completely occupied instead of the Cr t_{2g} states for which only the majority states are occupied. This leads to an extended reorganization of the p charge of the As(Se) impurity p states and the charge is now mainly localized in intense narrow picks located at around -3 eV and just below or above the gap. In the case of As impurities at Cr sites the unoccupied spin-down states are well above the Fermi level but the neighboring As sites show a small spin-down pick pinned exactly at the Fermi level. When the As impurity atom occurs at a Void1 site the difference in the impurity cluster leads to a narrow spin down pick just above the Fermi level. Thus the half-metallicity is preserved although the gap shrinks. In the case of CrSe, Se atoms have one electron more than As. When we create the impurity atom, its charge is no more accommodated in transition-metal bands [8] leading to an extra minority pick. When the Se impurity is located at the Void1 site the Fermi level is just above the gap while when the Se impurity is

located at the Cr site the Fermi level falls within this pick completely destroying half-metallicity. But our results are for the InAs lattice constant. If we contract the lattice constant we push the p states higher in energy and when we expand it we push them lower in energy [8] and thus it is very probable that the Fermi level falls within these picks completely destroying the half-metallic character of the parent compounds. The As(Se) nearest neighbors are affected by the As(Se) impurity since now they have three Cr atoms and one sp atom as nearest neighbors and a small fraction of their p charge moves to the same energy region with the picks of the impurity atom.

We should also discuss briefly the spin moments presented in table 4. The impurity atoms have positive spin moments contrary to the sp atoms at the perfect bulk compounds where they have negative spin moments. This is due to the difference in the hybridization, as we referred to above, which leads to occupancy of antibonding p spin-up states. The only exception is the Se impurity atom at the Void1 site which has a negative spin moment. The sp atoms which are the nearest neighbors of the impurity have spin moments very close to the bulk case since the DOS are also similar. Thus no general rule or conclusion can be drawn for the case of sp atom impurities at Void1 and Cr sites since depending on the chemical type of the sp atom and the lattice constant the Fermi level can fall within a minority spin pick destroying the half-metallicity.

4. Other impurities

To conclude our study on single impurities we will also present our results when the Cr or sp impurities appear at next-nearest neighbors sites. When these impurities are created the impurity atoms keep the same local environment as in the bulk compound (same nearest neighbors)

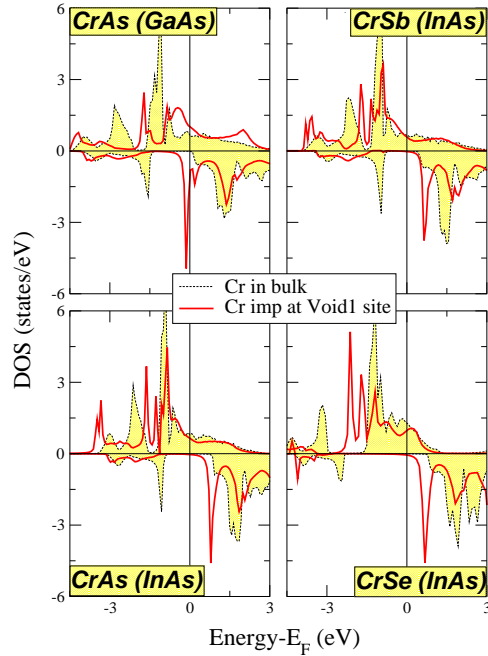


Figure 5. (Color online) Cr-resolved DOS for the case of Cr impurity atoms at Void1 sites (solid red lines) for all four compounds under study with respect to the perfect bulk case (dashed black line with shaded region).

since as we have mentioned in section 1 Cr and Void1 sites have 4 sp and 4 Void2 sites as nearest neighbors (sp and Void2 sites have 4 Cr and 4 Void1 site as nearest neighbors). In figure 5 we present the DOS for the case of Cr impurity atoms at Void1 sites for all four compounds with respect to the Cr atoms in the perfect compounds. Although the local environment remains unchanged, the impurity cluster as can be seen in table 2 is different. This leads again to a shift of the e_g minority spin states towards lower energies. While in the perfect compounds the e_g and t_{2g} minority states overlap, in the case of impurities the e_g states create a new pick just below the t_{2g} states. For the compounds at the InAs lattice constant the presence of the pick leads

Table 4. Atom-resolved spin magnetic moments for several cases of impurities. "imp" stands for impurity, "nn" stands for nearest neighbor atoms (1st neighbors) and "nnn" for next-nearest neighbors (2nd neighbors). In the last part on the As(Sb,Se)-Void1 atomic swaps we present the minimum and maximum values of Cr nn spin moments (see text for explanation).

	CrAs(GaAs)	CrAs(InAs)	CrSb(InAs)	CrSe(InAs)
As(Sb,Se) impurity at Cr site				
sp imp	0.0627	0.133	0.177	0.226
As nn	-0.162	-0.232	-0.119	-0.067
As(Sb,Se) impurity at Void1 site				
sp imp	0.005	0.146	0.155	-0.572
As nn	-0.140	-0.233	-0.119	-0.210
Cr nnn	2.952	3.439	3.387	3.717
Cr impurity at Void1 site				
Cr imp	3.038	3.505	3.441	3.993
As nn	-0.206	-0.295	-0.205	-0.187
Cr nnn	2.968	3.433	3.338	3.910
As(Sb,Se) impurity at Void2 site				
sp imp	-0.169	0.455	0.374	-0.430
Cr nn	2.583	3.408	3.322	3.595
As nnn	-0.200	-0.247	-0.166	-0.161
Void impurity at Cr site				
Void imp	-0.065	-0.110	-0.102	-0.019
As nn	-0.314	-0.569	-0.353	-0.233
Void impurity at As(Sb or Se) site				
Void imp	0.367	0.296	0.285	0.355
Cr nn	3.502	3.731	3.576	4.063
As(Sb or Se)-Void1 atomic swaps				
sp imp	-0.027	0.156	-0.232	-0.469
Void1 imp	0.264	0.262	0.178	0.232
Cr nn	3.195	3.737	3.579	3.854
	3.532	3.777	3.603	4.059

to a shrinking of the gap but the half-metallicity is preserved. But when we contract the lattice, as for CrAs at the GaAs lattice constant, the Fermi level is located within the minority e_g pick since the Fermi level is already at the right edge of the gap for the perfect bulk compound. The spin moments as can be seen in table 4 are very close to the bulk values and thus the no conclusion can be drawn from the spin magnetic moments. Cr impurities at Void1 sites do not affect the half metallicity only if the Fermi level is located at the lower-energy edge or the middle of the gap.

We will now proceed with the case of sp impurities at Void2 sites. We present for all four compounds the DOS of the sp impurity and its closest Cr neighbor in figure 6. The situation is also complex as in the case of sp impurities at Cr or Void1 sites. The p states are again reorganized in narrow picks and the half-metallic character depends on the exact position of these picks with respect to the Fermi level. In the case of CrAs at GaAs or InAs lattice constant, the Fermi level is located exactly just below or just above such a minority spin pick. An image of the states in this pick survives also for the

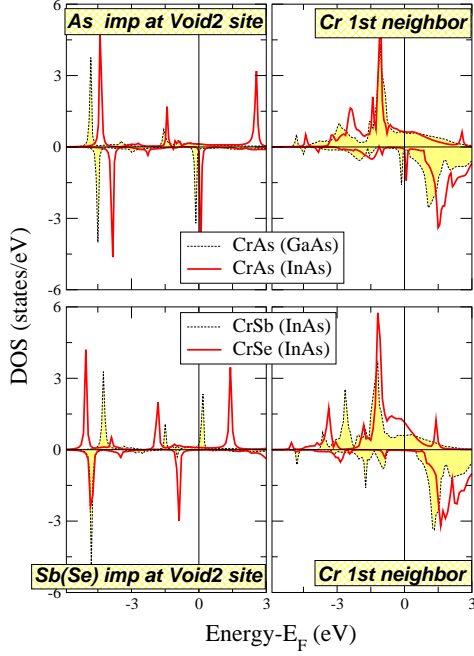


Figure 6. (Color online) As(Sb or Se)-resolved DOS for the case of As(Se) impurity atoms at Void2 sites and their 1st Cr neighbors.

Cr neighbors which now have 5 instead of 4 sp atoms as nearest neighbors and the hybridization effect for the t_{2g} states is more intense leading also to smaller Cr spin moments with respect to the bulk case as can be seen in table 4. In the case of CrSb and CrSe these states are located lower in energy due to the larger Coulomb repulsion between the p electrons (Sb is isovalent to As but has also the 5d states occupied while Se has one electron more than As) and the half-metallicity is preserved.

Finally we should also discuss the case of Void impurities at Cr or sp sites. We do not present the DOS since it is almost identical to the bulk cases for the neighboring atoms. This is also reflected on the spin moments presented in table 4. When we create the Void impurity at the sp site, the Cr nearest neighbors have now 3 instead of 4 neighboring sp

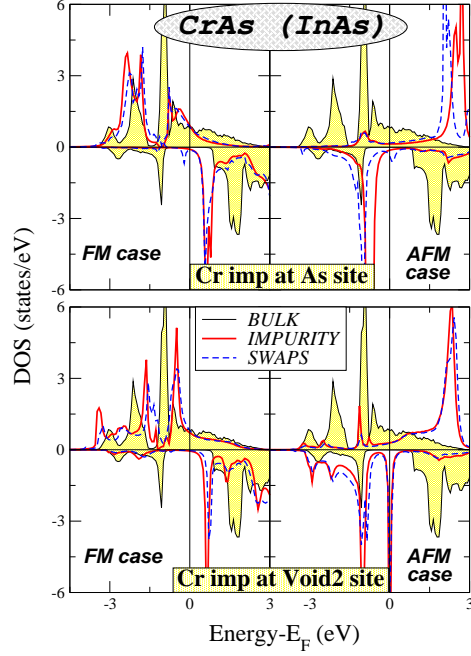


Figure 7. (Color online) For the case of CrAs in the InAs lattice constant, we present the Cr-DOS (for both AFM and FM cases) for both Cr impurity atoms at As site (solid red line) and Cr-As atomic swaps (dashed blue line) in the upper panel, and for both Cr impurity atoms at Void2 sites (solid red line) and Cr-Void2 atomic swaps (dashed blue line) in the lower panel. With the solid black line with the shaded region we present the perfect bulk case.

atoms and thus the hybridization effect is smaller leading to slightly larger Cr spin moments. The same occurs also when the Void impurity is located at a Cr site and the absolute value of the spin magnetic moment of the neighboring sp atoms increases slightly. The width of the gap remains unchanged by the Void impurities at Cr or sp sites and half-metallicity is not altered.

5. Atomic swaps

In the last section we will present our results on the atomic swaps. As we mentioned in section 1 we performed calculations for the case of atomic swaps between nearest neighboring sites (i) Cr-sp atom, (ii) Cr-Void2, and (iii) sp atom-Void1. Atomic swaps present properties very similar to the properties of the single impurities. We will start our discussion from the case of swaps involving Cr atoms. For both Cr-sp atom and Cr-Void2 swaps we were able to converge two solutions for the InAs lattice constant: a FM and an energetically-favorable AFM coupling of the Cr impurity with respect to its neighboring atoms. For CrAs at the GaAs lattice constant the distance between the Cr atoms is very short to stabilize a FM solution and we were able to converge only the AFM solution. In table 3 we present the spin moments of the impurity atoms for all cases. In the case of swaps each Cr impurity atom has 3 Cr atoms and one sp atom as nearest neighbors while in the case of a Cr single impurity the Cr-impurity atoms had 4 Cr atoms as first neighbors. Since the t_{2g} states of the Cr atoms hybridize strongly with the p states of the sp atoms, this leads to an increased hybridization in the case of the atomic swaps and thus to smaller absolute values of the spin magnetic moments of the Cr atoms in both the FM and AFM cases. In figure 7 we present the Cr DOS for the Cr impurity atoms at both As and Void2 sites for both FM and AFM cases in the case of CrAs at the InAs lattice constant, and we compare the perfect bulk case, the single impurity case discussed in section 2 and the swaps case. Overall the DOS of the Cr impurity atom only scarcely changes between the single impurity and swaps cases. In the case of the Cr impurity at the Void2 site the e_g states in the AFM solution are pinned at the Fermi level destroying the half-metallicity as in the case of single impurity. When the

Cr impurity atom is located at the As site there is an extra minority pick at the Fermi level in the case of atomic swaps. To understand its origin we should keep in mind that also an As atom moves at a Cr site in the case of swaps and as we can see in the lower left panel of figure 4 already in the case of a single As impurity at a Cr site the neighboring atoms present a small DOS at the Fermi level which destroys the half-metallicity. In the case of Cr-As swap, the As impurity atom has one Cr atom and three As atoms as nearest neighbors and this pick is present destroying the half-metallicity. Thus the energetically favorable AFM case of Cr-As and Cr-Void2 swaps induces states within the gap.

Finally we should also shortly discuss the third case of atomic swaps: sp-Void1. In table 4 we present the spin magnetic moments at the Void1 and sp impurity sites. The nearest Cr atoms are no more equivalent and thus their total spin moment varies between the values given in the table. We do not present the DOS since results are similar to the case of single sp impurities at Void1 sites presented in section 3. There is a very narrow intense pick near the Fermi level as in the upper panel of figure 4 which can lead to the loss of half-metallicity depending on its exact position with respect to the Fermi level which is influenced from the electronegativity of the sp atom and the lattice constant.

6. Conclusion

We have studied using the Korringa-Kohn-Rostoker method the appearance of single impurities and atomic swaps in the half-metallic CrAs, CrSe and CrSb alloy crystallizing in the zinc-blende structure. Although it was found that Cr antisites at sp sites lead to half-metallic ferrimagnetism, we found that the situation is much more complex. Cr single impurities at sp or Void2

(see figure 1 for the structure) sites can couple either antiferromagnetically (which is the energetically favored) or ferromagnetically (in case of large lattice constants) to their nearest Cr neighbors. Although in most cases the gap survives there are cases like the case of Cr impurities at Void2 sites in CrSe where the e_g minority-spin states are pinned exactly at the Fermi level. Cr impurities at Void1 sites lead to a shift of the unoccupied minority e_g states lower in energy and when the Fermi level is near the right edge of the gap in the perfect compound the half-metallicity is lost. sp impurities at Cr, Void1 or Void2 sites lead to a redistribution of the p charge and they are likely to induce new impurity states at the Fermi level. The appearance of void impurities at Cr and sp atoms is the only case where the gap is not affected at all. Finally we studied also the case of atomic swaps between nearest neighbors. We found that in the case of Cr-sp and Cr-Void2 swaps, the presence of the sp impurity atom leads to new minority states pinned at the Fermi level even in the cases where the half-metallicity was preserved for single Cr impurities. Void1-sp swaps show behavior similar to the single sp impurities at Void1 sites.

Although impurity states are localized in space around the impurity atoms and very fast we regain the bulk behavior, their interaction can lead to wide impurity bands within the gap and thus the loss of the half-metallic character. Only void impurities at Cr and sp sites and Cr impurities at sp sites (as long as no swap occurs) keep the half-metallic character of the perfect alloys. Our results suggest that for CrAs alloys in the zinc-blende structure to be implemented in spintronic devices, the prevention of the defects creation is imperative.

References

- [1] Žutić I, Fabian J and Das Sarma A 2004 *Rev. Mod. Phys.* **76** 323
- [2] de Groot R A, Mueller F M, van Engen P G and Buschow K H J 1983 *Phys. Rev. Lett.* **50** 2024
- [3] Galanakis I, Dederichs P H and Papanikolaou N 2002 *Phys. Rev. B* **66** 134428
- [4] Galanakis I, Dederichs P H, and Papanikolaou N 2002 *Phys. Rev. B* **66** 174429; Weht R and Pickett W E 1999 *Phys. Rev. B* **60** 13006
- [5] Soulen Jr R J, Byers J M, Osofsky M S, Nadgorny B, Ambrose T, Cheng S F, Broussard P R, Tanaka C T, Nowak J, Moodera J S, Barry A and Coey J M D 1998 *Science* **282** 85; Parker J S, Watts S M, Ivanov P G, and Xiong P 2002 *Phys. Rev. Lett.* **88** 196601
- [6] Akinaga H, Manago T, and Shirai M 2000 *Japan. J. Appl. Phys.* **39** L1118
- [7] Deng J J, Zhao J H, Bi J F, Zheng Y H, Jia Q J, Niu Z C, Wu X G and Zheng H 2006 *Chin. Phys. Lett.* **23** 493; Akinaga H and Mizuguchi M 2004 *J. Phys.: Condens. Matter* **16** S5549; Zhao J H, Matsukura F, Takamura K, Abe E, Chiba D, and Ohno H 2001 *Appl. Phys. Lett.* **79** 2776; Akinaga H and Mizuguchi M 2004 *J. Phys.: Condens. Matter* **16** S5549
- [8] Galanakis I and Mavropoulos Ph 2003 *Phys. Rev. B* **67** 104417
- [9] Galanakis I 2002 *Phys. Rev. B* **66** 012406
- [10] Zhao Y J and Zunger A 2005 *Phys. Rev. B* **71** 132403; Miao M S and Lambrecht W R L 2005 *Phys. Rev. B* **72** 064409; Shi L J and Liu B G 2005 *J. Phys.: Condens. Matter* **17** 1209
- [11] Shirai M 2004 *J. Phys.: Condens. Matter* **16** S5525; Shirai M, Seike M, Sato K and Katayama-Yoshida H 2004 *J. Magn. Magn. Mater.* **272-276** 344
- [12] Nakamura K, Kato Y, Akiyama T, Ito T, and Freeman A J 2006 *Phys. Rev. Lett.* **96** 047206
- [13] Xie W H, Xu Y Q, Liu B G, and Pettifor D G 2003 *Phys. Rev. Lett.* **91** 037204; *idem* *Phys. Rev. Lett.* **91** 219901 (erratum)
- [14] Chioncel L, Mavropoulos P, Ležaić M, Blügel S, Arrighoni E, Katsnelson M I, and Lichtenstein A I 2006 *Phys. Rev. Lett.* **96** 197203
- [15] Mavropoulos P, Galanakis I, and Dederichs P H 2004 *J. Phys.: Condens. Matter* **16** 4261; Fong C Y, Qian M C, Pask J E, Yang L H, and Dag S 2004 *Appl. Phys. Lett.* **84** 239
- [16] Şaşıoğlu E, Galanakis I, Sandratskii L M, and Bruno P 2005 *J. Phys.: Condens. Matter* **17** 3915

- [17] Ležaić M, Mavropoulos P, Enkovaara J, Bihlmayer G, and Blügel S 2006 *Phys. Rev. Lett.* **97** 026404; Chioncel L, Katsnelson M I, de Wijs G A, de Groot R A, and Lichtenstein A I 2005 *Phys. Rev. B* **71** 085111; Skomski R and Dowben PA 2002 *Europhys. Lett.* **58** 544
- [18] Mavropoulos Ph and Galanakis I 2007 *J. Phys.: Condens. Matter* **19** 315221
- [19] Galanakis I, Özdoğan K, Şaşıoğlu E, and Aktas B 2006 *Phys. Rev. B* **74** 140408(R)
- [20] Koepernik K and Eschrig H 1999 *Phys. Rev.* **59** 1743; Koepernik K, Velicky B, Hayn R and Eschrig H 1998 *Phys. Rev. B* **58** 6944
- [21] van Leuken H and de Groot R A 1995 *Phys. Rev. Lett.* **74** 1171; Özdoğan K, Galanakis I, Şaşıoğlu E, and Aktas B 2006 *J. Phys.: Condens. Matter* **18** 2905; Şaşıoğlu E, Sandratskii L M, and Bruno P 2005 *J. Phys.: Condens. Matter* **17** 995
- [22] Özdoğan K, Galanakis I, Aktas B, and Şaşıoğlu E (2008) *J. Magn. Magn. Mater.* **320** 197.
- [23] Korhonen T, Settels A, Papanikolaou N, Zeller R, and Dederichs P H 2000 *Phys. Rev. B* **62** 452
- [24] Papanikolaou N, Nonas B, Heinze S, Zeller R, and Dederichs P H 2000 *Phys. Rev. B* **62** 11118